Accident Analysis and Prevention 129 (2019) 94–107

Contents lists available at ScienceDirect

Accident Analysis and Prevention

journal homepage: www.elsevier.com/locate/aap

Potential benefits of controlled vehicle braking to reduce pedestrian ground contact injuries

Tiefang Zou[a,b,c], Shi Shang[b], Ciaran Simms[b,*]

[a] School of Automobile and Mechanical Engineering, Changsha University of Science and Technology, Changsha, 410114, China
[b] Centre for Bioengineering, School of Engineering, Trinity College Dublin, Dublin, 2, Ireland
[c] Key Laboratory of Safety Design and Reliability Technology for Engineering Vehicle, Hunan Province, 410114, China

ARTICLE INFO

Keywords:
Pedestrian vehicle accident
Ground contact
Braking
Weighted injury cost

ABSTRACT

Protecting struck pedestrians during the ground contact phase has been a challenge for decades. Recent studies have shown how ground related injury is influenced by pedestrian kinematics. In this paper we further developed this approach by assessing the potential of controlling vehicle braking to reduce pedestrian ground contact injuries. Applying a recently proposed Simulation Test Sample, a series of simulations were run using the MADYMO software environment. The approach considered 6 vehicle shapes, 4 pedestrian models, 3 impact velocities and 2 pedestrian gaits and each case was considered with two different vehicle braking approaches. The first was full braking, while the second applied controlled braking, for which a strategy based on pedestrian kinematics was applied. The effect of vehicle braking was evaluated using the Weighted Injury Cost (WIC) of overall pedestrian injuries and the pedestrian-ground impact velocity change. The proximity of the vehicle and pedestrian at the instant of ground contact was also evaluated to assess the potential of future vehicle based intervention methods to cushion the ground contact. Finally real-world videos of pedestrian collisions were analyzed to estimate the available free vehicle stopping distances. Results showed substantial median reductions in WIC and head impact velocity for all vehicle shapes except the Van. The proximity of the pedestrian to the vehicle front at the instant of ground contact under controlled braking is less than 1.5 m in most cases, and the required stopping distance for the vehicle under controlled braking was within the available stopping distance estimated from the video footage in about 74% of cases. It is concluded that controlled braking has significant potential to reduce the overall burden of pedestrian ground contact injuries, but future efforts are required to establish an optimized braking strategy as well as a means to handle those cases where controlled braking is not beneficial or even harmful.

1. Introduction

Pedestrians are among the most vulnerable road users and the World Health Organization estimates about 270,000 pedestrian fatalities occur annually following road traffic collisions (WHO, 2013). Pedestrian injuries result from both the first contact with the vehicle and the secondary contact with the ground. Many studies have found that injuries from the vehicle are more severe and more frequent (Otte and Pohlemann, 2001; Kendall et al., 2006; Badea-Romero and Lenard, 2013 Zou et al., 2017). Nonetheless, a recent study of collisions below 40 km/h (Shang et al., 2018a) found that two thirds of the injury costs would be eliminated if ground contact could be prevented. However, despite this motivation, there are no accepted interventions to reduce ground contact injuries.

Pedestrian ground contact injuries are not easily predictable (Simms and Wood, 2006a; Tamura and Duma, 2011; Tamura et al., 2014) as the outcome is highly influenced by the impact speed, vehicle front-end shape, pedestrian heights, gaits, speeds and the body angle at the instant of ground contact (Simms and Wood, 2006a; Simms et al., 2011; Tamura and Duma, 2011; Hamacher et al., 2012; Peng et al., 2012; Tamura et al., 2014; Li et al., 2015; Nie and Zhou, 2016 Yin et al., 2017). To better understand ground related injury, different impact mechanisms (Crocetta et al., 2015) and pedestrian rotation angle ranges (PRARs) (Shi et al., 2018; Han et al., 2019) have been proposed to relate vehicle front-end shape, collision speed and pedestrian characteristics to head-ground impact speed. Most studies used MADYMO multibody simulations, though some have applied finite element approaches (Tamura and Duma, 2011; Tamura et al., 2014) or videos (Han et al., 2019) and some very early studies used dummies and cadavers (Stcherbarcheff et al., 1975 and Cavallero et al., 1983). None of

* Corresponding author.
E-mail address: csimms@tcd.ie (C. Simms).

https://doi.org/10.1016/j.aap.2019.05.008
Received 7 January 2019; Received in revised form 11 April 2019; Accepted 7 May 2019
Available online 24 May 2019

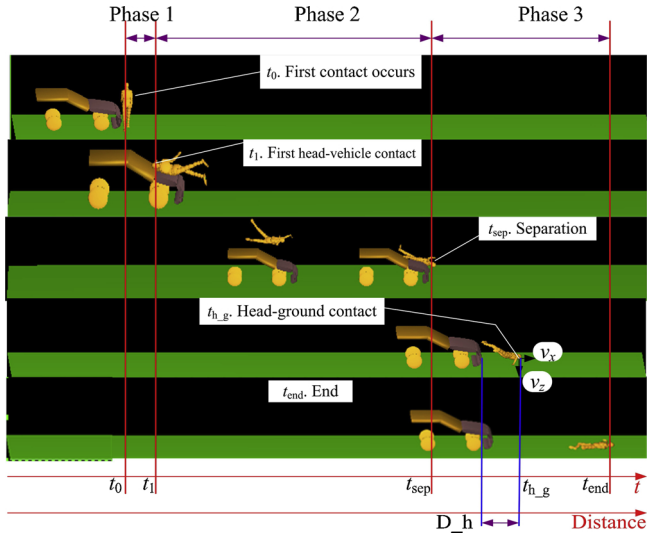

Fig. 1. The phases of a vehicle-pedestrian collision: first contact occurs at t_0, and the head to vehicle contact first occurs at t_1. Depending on vehicle braking and collision speed, the pedestrian will continue interacting with the vehicle before separating from it at t_{sep}. After separation has commenced, full braking is required to prevent pedestrian run-over.

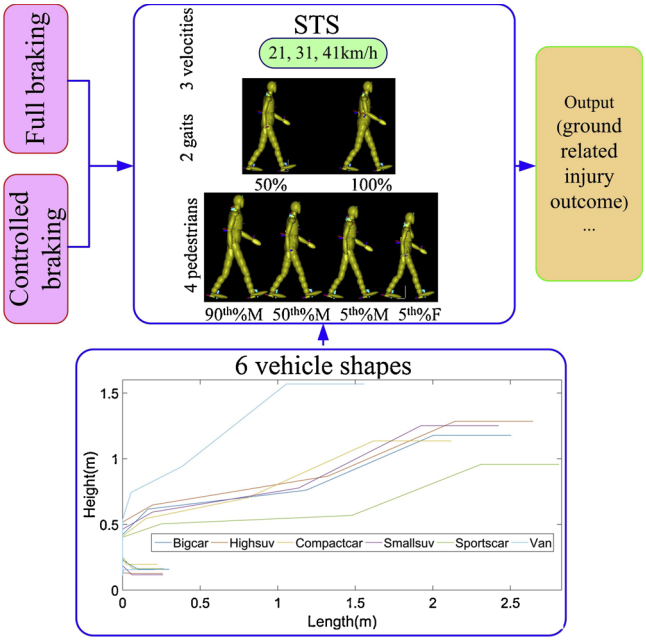

Fig. 2. Overview of simulations to assess effect of vehicle braking on ground related injury outcome (2 braking methods × 6 vehicle shapes × 4 pedestrian models × 3 impact velocities × 2 pedestrian gaits).

the numerical models are validated for ground contact due to a shortage of experimental data, though this is now being addressed (Shang et al., IRCOBI 2018b).

Few studies have focused on approaches to reduce pedestrian ground contact injury. Otte et al. (Otte and Pohlemann, 2001) suggested external airbags and Google (Google, 2016) recently proposed an adhesive method to prevent ground contact. Li et al. (Li et al., 2017a) proposed a framework for vehicle front-end shape optimization and presented vehicle shapes for overall pedestrian protection (partially including ground contact). However, none of these solutions have been implemented, so their efficacy in the field remains unknown.

In this paper, it is hypothesized (following a review of preliminary simulations) that the severity of pedestrian ground contact can be reduced by controlling vehicle braking in wrap trajectory cases after the primary impact with the pedestrian is substantially complete, see Fig. 1. The purpose of controlled vehicle braking is to change the kinematics of the pedestrian by using additional contact(s) with the vehicle to reduce the vertical speed of pedestrian ground contact.

It is further hypothesized that in most cases the available vehicle stopping distance is sufficient to permit controlled braking for pedestrian protection without inducing a further vehicle collision. The first hypothesis is tested by multibody modelling and the second by multibody modelling and analysis of real-world videos.

2. Methods

2.1. Design of experiments

Pedestrian ground contact injuries for a given vehicle stiffness depend on vehicle shape and impact speed and pedestrian height and gait. Li et al. (Li et al., 2016a) proposed a Simulation Test Sample (STS) in which these parameters are all considered. An STS including sixty impact scenarios (6 impact speeds × 5 pedestrian heights × 2 pedestrian gaits) was applied as this efficiently predicted injury distributions (Li et al., 2016b, a; Li et al., 2018). This STS approach was selected to test the effects of controlled braking in this paper.

Li et al. applied impact speeds of 21, 31, 41, 50, 61 and 70 km/h based on GIDAS data (Li et al., 2016b,a). However, above about 40 km/h vehicle contact injuries are much more important than ground contact injuries (Simms and Wood, 2009; Feng et al., 2013; Yin et al., 2017). Accordingly, 21, 31 and 41 km/h were the speeds considered in this study, and this reduced range still covers a large majority of actual pedestrian impacts (Li et al., 2017a; Li, 2017b; Guillaume et al., 2015; Eubanks et al., 2018).

Li et al. applied 5 pedestrian models in the STS: a 6 year old (6YOC), 5th% female (5th%F), 5th% male (5th%M), 50th% male (50th%M) and 90th% male (90th%M). However, as the 6YOC model is too short to achieve a wrap trajectory, it was excluded here. Similar to Li et al., 2016a, 2 pedestrian gaits (50% and 100%) were considered.

The 6 vehicle shapes used by Crocetta et al. (Crocetta et al., 2015) were applied to represent a Sports car, Compact car, Big car, Small SUV, High SUV and a Van. To test the hypothesis that controlled braking is beneficial for ground contact, each collision scenario was simulated with full braking and also with controlled braking and the resulting ground related kinematics and injury predictions were compared on a case by case basis, see Fig. 2.

A total of 288 simulations (2 braking methods × 6 vehicle shapes × 4 pedestrian models × 3 impact velocities × 2 pedestrian gaits) were conducted using the multi-body simulation software MADYMO. In each simulation, similar to previous studies, the friction coefficients of pedestrian to vehicle and ground contact were respectively set to 0.3 and 0.6 respectively. A single stiffness level for each vehicle front structure was considered (see Appendix A).

2.2. Controlled braking

Since the goal is to determine whether controlled braking can in principle be beneficial, only a single controlled braking method is evaluated here. Fig. 3 shows the braking pulse: at t_0 the pedestrian first contacts the vehicle and t_1 is the first head-vehicle contact time. The vehicle is fully braked until t_1 to minimize the vehicle-head impact velocity. After t_1, the pedestrian velocity is approximately equal to the vehicle velocity (Brach and Brach, 2005; Zou et al., 2011) and further contacts between the vehicle and the pedestrian due to reduced braking are not significant from the perspective of injury causation. Rather, these additional contacts serve to interrupt the downward trajectory of the pedestrian under gravity, ultimately reducing the speed of contact with the ground. Hence, braking is reduced to 0 at t_1, with a lag time of

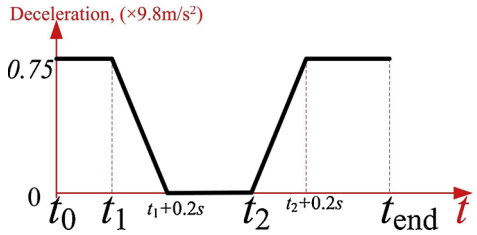

Fig. 3. Curve of the deceleration of the controlled braking method.

0.2 s (Datentechnik, 2013) until t_2, when full braking is resumed (accounting for lag time) to avoid pedestrian run-over.

Considering that t_1 can be detected with modern sensors, determining t_2 becomes the core problem. In future we will assess efficient ways to find t_2, but here we focus on establishing whether significant potential benefits could accrue to pedestrians by controlled vehicle braking. Accordingly, t_2 was determined sequentially by running each scenario with different braking conditions. The first full braking simulation was used to detect t_1. A second controlled braking simulation applied reduced braking between t_1 and t_2 fixed at 1.6 s. From this, the final t_2 (used in the third simulation) was determined by consideration of the pedestrian kinematics. Rules used for determining the final t_2 are:

Rule 1. In some cases, the pedestrian falls to the side of the vehicle and there is then no benefit from controlled braking. Hence t_2 is set to $t_2 = t_1 + 0.2$ s.

Rule 2. For most simulations, the time when the height of the pelvis, head or torso is lower than the bonnet leading edge (BLE) height is set to t_2 (equivalent to t_{sep} in Fig. 1). Future vehicles should be readily able to detect this.

Rule 3. For other simulations, feet contact with the windshield or the roof causes the pedestrian and vehicle to continue to interact, resulting in a large t_2, but this needs to be balanced against the available stopping distance. Hence, if $t_2 > 1.4$ s, a new value $t_2 = t_1 + 0.2$ s $+ a_t < 1.4$ s is reassigned to t_2, where a_t is an empirical parameter. After numerous attempts, we found that $a_t = 0.45$ s yielded favourable results.

The constraint of 1.4 s was calculated according to the available stopping distance as follows. A convenience sample of 100 pedestrian collision cases was selected from the internet (Youku, YouTube, etc) using search engines Baidu and Google (keywords included “pedestrian accident”, “pedestrian accident video”, “car pedestrian accident” and “pedestrian crash”). The Approximate Available Stopping Distance (AASD) is the minimum available vehicle travel distance (assuming a forward trajectory) before a further conflict occurs (eg. another vehicle, an intersection or another pedestrian), and this was estimated visually. Table B1 in Appendix B shows the average AASD is ≈ 20 m. This was selected as a constraint (20 m) and the maximum impact velocity (41 km/h) was used to establish an upper limit for t_2. Analysis of 34 accident cases presented by Zou et al., 2017 was first used to estimate t_1 = 0.14 s at 41 km/h (see section 1 in Appendix B). A MADYMO simulation of a Compact Car striking a 50th % male pedestrian was then applied to estimate the maximum value of t_2 using the method shown in Fig. 3 to control braking. Fig. B2 in Appendix B shows the maximum value of t_2 = 1.4 s for a wrap trajectory case with a collision speed of 41 km/h, and this was used to constrain the maximum value of t_2 to 1.4 s.

2.3. Evaluation indices for ground contact

Three indices are proposed to estimate the effect of applying controlled braking on pedestrian ground contact injuries.

A The Weighted Injury Cost (WIC) proposed by Li et al. (Li et al., 2017a) was employed to combine injuries to the head (HIC), thorax (TTI), pelvis (impact force), lower limbs (bending moment) and knees (bending angle). The predicted AIS injury levels were converted to Injury Cost (IC) and the WIC was calculated by weighting the frequency of occurrence of the different cases, similar to Li, 2017b.

B The vertical component of the velocity change of the pedestrian’s head during ground impact (ΔV_z) was assessed. Since the pedestrian-ground contact model is not validated (Crocetta et al., 2015; Yin et al., 2017; Li et al., 2017a; Shi et al., 2018), this approach partially offsets uncertainties associated with the HIC calculation which depends strongly on the characteristics of the ground contact. The predicted head-ground contact force and vertical position of the head were used to find the head-ground contact time t_{h_g}, which was used together with the head vertical velocity to find the head-ground contact time interval and hence ΔV_z.

C The horizontal distance between the head at first contact with the ground and the front of the vehicle (D_h). If this is sufficiently small (< 1.5 m), it may be possible for external airbags to(Pipkorn et al., 2007) provide protection during pedestrian-ground contact.

2.4. Analysis approach

The 288 simulations were divided into two groups. The vehicle is fully braked in the first group (“full brake”), while in the second group vehicle braking is controlled (“contr.-brake”). The two groups are compared (WIC, ΔV_z & D_h) with vehicle shape or impact velocity as the independent variable and the Wilcoxon Matched pair tests (at the 5% significance level) was used to test for mean differences. The emphasis is on trends rather than magnitudes to reduce the effects of uncertainties in ground contact modelling.

3. Results

3.1. The vehicle stopping distance

Fig. 4 shows box plots of vehicle stopping distance at the three chosen impact velocities for the fully braked versus the controlled braking groups. Controlled braking substantially increases the stopping distance, but due to the definition of t_2 in section 2.2 in all cases it is less than 20 m.

If the upper quartile vehicle stopping distance for each speed category in Fig. 4 is selected as a limit, then the requisite stopping distance for 21, 31 and 41 km/h for controlled braking is 4, 9 and 14.5 m respectively. Considering 21, 31 and 41 km/h as the mean of impact speed intervals [16–25], [26–35] and [36–45] km/h respectively (Li et al., 2017a) and comparing to the estimated required stopping distance in the real collision cases in Appendix Table B1, the following was

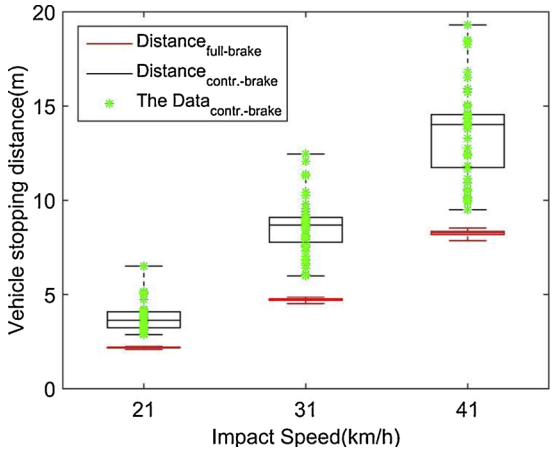

Fig. 4. Box plots of vehicle stopping distance versus the impact speed for full braked and controlled braking cases.

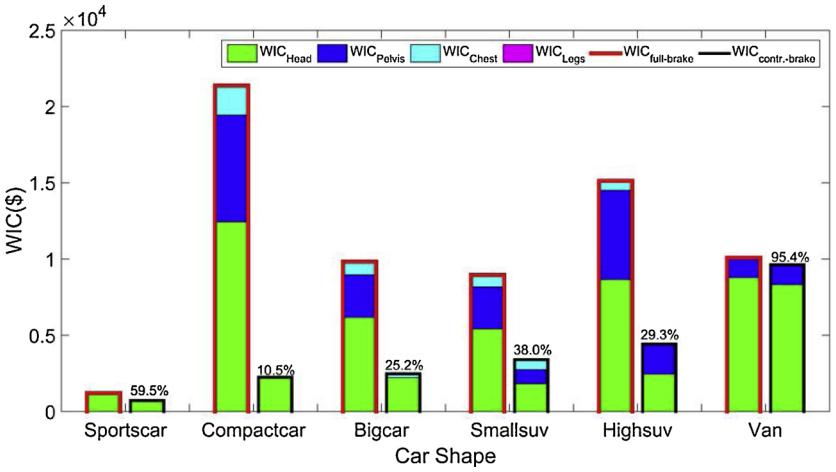

Fig. 5. Bar plots of WIC for full braking versus controlled braking for each vehicle shape: the subscripts indicate the relevant body region. The bar with a red bound is the fully braked group while the bar with the black bound is the controlled braking group. The percentages refer to the proportion of $WIC_{contr.-brake}/WIC_{full-brake}$. (For interpretation of the references to colour in this figure legend, the reader is referred to the web version of this article).

observed: for impact speeds less than 26 km/h, the required stopping distance is less than the estimated available stopping distance in 18 out of 19 cases. For 26–35 km/h cases, the proportion is 20 out of 30 cases and for 36–45 km/h the proportion is 19 out of 28 cases. In total 57/77 = 74% cases lie within the upper quartile limit for required stopping distance.

3.2. The WIC

Fig. 5 shows predicted WIC versus car shape. In all cases controlling the braking reduced the WIC but the effect ranges from negligible to considerable. In general, the biggest effect is on the WIC_{Head}, then the WIC_{Pelvis}, while the WIC_{Legs} is zero in all cases (the latter indicating a limitation in the modelling). The influence of braking depends strongly on vehicle shape. For the compact car, big car and high SUV, very substantial benefits are predicted. In contrast, for the Van there is almost no benefit, largely because the wrap trajectory is largely absent for this vehicle shape.

3.3. The ΔV_z

Fig. 6 shows the predicted reduction in ΔV_z for controlled braking compared to full braking. For all vehicle shapes except the van, the median ΔV_z is reduced (average median reduction is ca. 1.2 m/s). However, the Wilcoxon matched pair test showed significant median difference of ΔV_z differences only for the high SUV and compact car. For the van ΔV_z is almost unchanged, again indicating that controlled braking is not beneficial for this vehicle shape. Despite the median improvement for the other vehicle shapes, in a small number of cases controlled braking increased the predicted head ground velocity substantially. These cases require further analysis in future. Similar conclusions can be found from the HIC data (see Appendix C).

3.4. The D_h

Fig. 7 shows distributions of D_h for the different vehicle shapes. This index shows the potential for external airbags to be effective in cushioning the ground contact. The distance D_h is substantially shortened for all vehicle categories by controlling the braking. The Wilcoxon matched pair test showed significant D_h differences between the 2 groups for all vehicle shapes except the big car and van. In the controlled braking group, if the protection scope of an external airbag is 1 m, potential protection could be provided in more than half of the cases. If the protection scope extends to 1.5 m, protection could be provided in most cases.

3.5. Kinematic response of the pedestrian

Fig. 8 shows the kinematic response of the pedestrian for a sample 41 km/h case of controlled braking versus full braking. The kinematic response is almost the same until about 1.1 s after initial contact. However, at 1135 ms, in the controlled braking case, the pedestrian contacts the vehicle again (this is predominantly a vertical contact), thereby ultimately reducing the downward velocity of the pedestrian at the instant of ground contact. This results in a lower HIC15 for the ground contact in the controlled braking case. However, in some

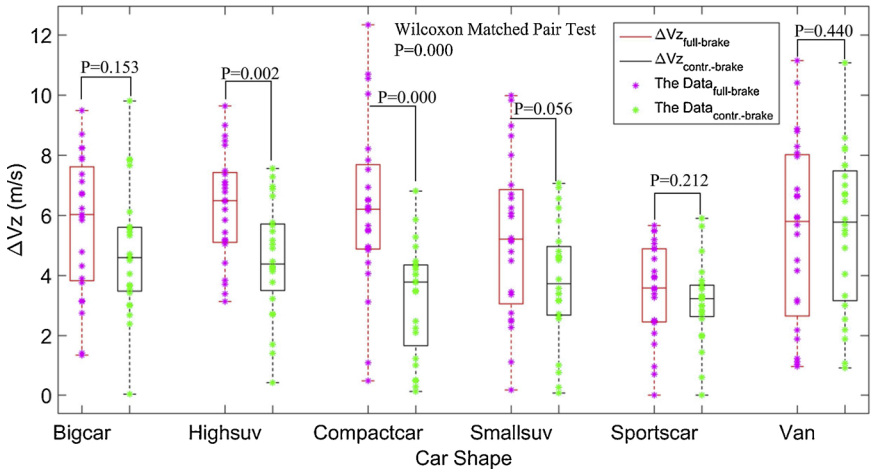

Fig. 6. The difference of ΔV_z for controlled braking compared to full braking for different vehicles shapes. Results of a Wilcoxon matched pair test are also sown.

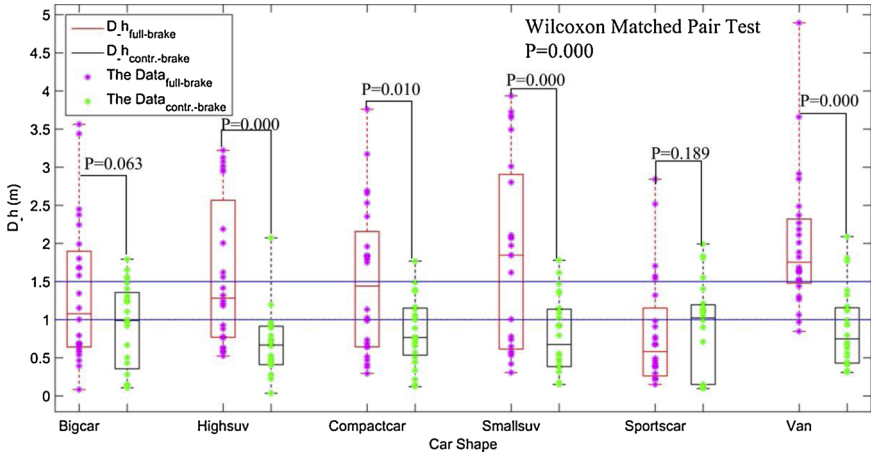

Fig. 7. Box plots of distance between the head at first contact with the ground and the front of the vehicle (D_h) for full braking versus controlled braking for different vehicle shapes.

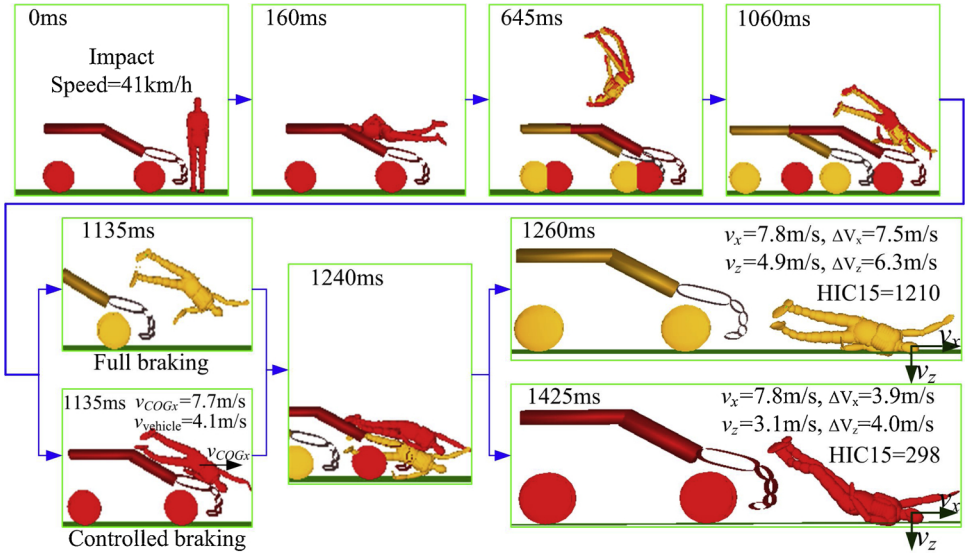

Fig. 8. Sample kinematic response for controlled (red) versus full (yellow) braking: v_x /v_z are the pedestrian head cg velocity components just prior to ground contact; ΔVx/z are the components of the pedestrian's head cg velocity change during ground impact; $v_{vehicle}$ is the vehicle velocity and v_{COGx} is the horizontal velocity of the pedestrian cg;). (For interpretation of the references to colour in this figure legend, the reader is referred to the web version of this article).

Table 1
Parameter sensitivity study to assess the effects of different STS combinations on predicted WIC for collisions with a compact car shape.

Group	STS size	Details
1	24	3 velocities (21, 31, 41 km/h) × 4 pedestrians × 2 gaits (50%, 100%)
2	48	3 velocities (21, 31, 41 km/h) × 4 pedestrians × 4 gaits (30%, 50%, 80%, 100%)
3	48	6 velocities (12.5, 18.5, 24.5, 30.5, 36.5, 42.5 km/h) × 4 pedestrians × 2 gaits (50%, 100%)
4	96	6 velocities (12.5, 18.5, 24.5, 30.5, 36.5, 42.5 km/h) × 4 pedestrians × 4 gaits(30%, 50%, 80%, 100%)

controlled braking cases the pedestrian orientation at the instant of ground contact results in higher ΔV_z, ΔV_x and v_x, v_z and hence HIC score (an example with a higher HIC is given in Fig. D1).

4. Discussion

Finding a practical solution to reducing pedestrian ground contact injuries has remained a challenge for many years. However, our modelling suggests that pedestrian ground contact can be improved by controlled braking. In particular, we found that the overall ground contact injuries and the velocity change in the head during ground contact can be reduced in many cases, while the distance between the pedestrian and the vehicle front at the instant of ground contact (D_h) is mostly less than 1.5 m. We also found the upper quartile of the required stopping distance for the vehicle under controlled braking was within the available stopping distance estimated from video footage of actual collisions in about 74% of cases.

This study shows two separate benefits of controlled vehicle braking: the severity of contact of the head and pelvis with the ground can be reduced and the proximity of the vehicle to the pedestrian at the ground contact is sufficient to make vehicle based interventions for cushioning the ground contact a possibility. In future, substantial additional effort is required to validate numerical models for ground contact injury prediction and to develop optimized strategies for controlling braking as only a single control strategy for braking was evaluated in this paper. However, to the best of our knowledge this paper provides the first quantitative evidence that controlled braking can often reduce pedestrian ground contact injury risk.

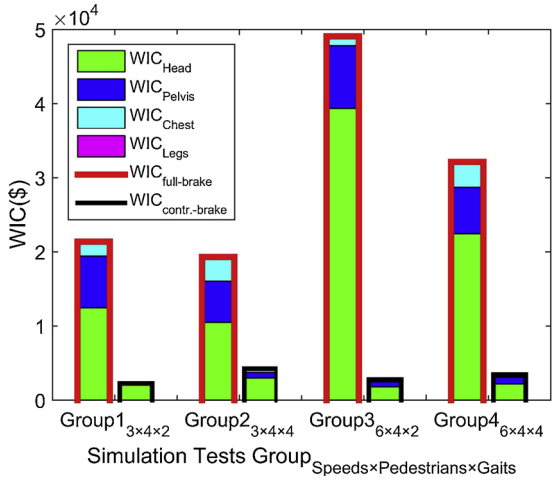

Fig. 9. WIC for full braking versus controlled braking for different STS combinations defined in Table 1.

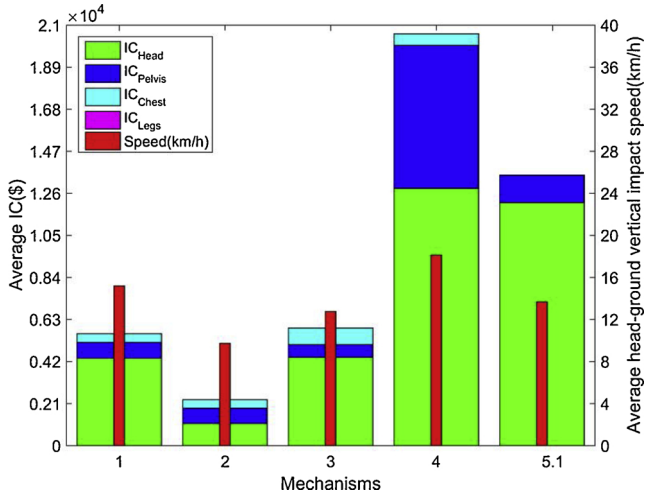

Fig. 10. Mean IC and vertical head ground speed versus mechanism for all simulations.

4.1. Limitations

Validation of computational modelling of ground contact remains a substantial challenge (Klug, 2018). Cadaver studies to provide validation data are ongoing (Shang, IRCOBI 2018b), but there remains considerable uncertainty in individual ground contact injury predictions and the absence of any predicted leg related injury cost is likely to be at least partly due to the absence of age related reductions in injury tolerance in the model. However our case-control approach applied to a wide range of collision scenarios, whereby the only variable in each comparison is the braking strategy, suggests the broad findings in this study are robust.

Related to this is whether 24 scenarios in the STS for each vehicle shape is a reasonable simplification of the broad range of pedestrian ground contact configurations. To address this, the most common vehicle shape “Compact car” was selected and results were evaluated for different STS combinations, see Table 1. Fig. 9 shows the predicted WIC for full braking versus controlled braking for the different STS combinations. The magnitude of the WIC is substantially influenced by the choice of STS combination and these results suggest that an upper limit of STS combinations for convergence has not been achieved. However, all STS combinations yield the same general effect of reduced WIC for controlled braking compared to the full braking. Accordingly, although future studies should focus on achieving a convergent STS sample size for quantifying ground contact injury predictions, it is unlikely that a larger STS sample size would substantially affect the braking results obtained in this paper.

To assess the potential benefits of controlled braking in the real-world vehicle fleet, the proportions of the different vehicle shapes are needed. According to (Guillaume et al., 2015), the proportion of vehicle shapes are: the wedge shape (2%), the box shape (8%), the pontoon shape (10%) and the trapezoidal shape (80%). From this we can define approximate proportions: Sports car (2%), Mid car (28%) + Big car (26%) + Small SUV (26%) = 80%, Big SUV (10%), van (8%). The resulting bar plots of WIC for controlled braking versus full braking as a function of impact velocity and pedestrian size are given in Appendix E. Fig. E1 shows the largest benefits are at 41 km/h, but at these speeds injuries from vehicle contact are likely to predominate. Fig. E2 shows controlled braking can be of benefit for all pedestrian sizes modelled.

The benefits of braking at each vehicle speed for the different vehicle shapes are shown in Appendix F. The van shows no real benefit (Fig. F1) and there are individual cases where controlled braking is not beneficial (Fig. F1 and Fig. F2), but mostly benefits are observed.

4.2. Biomechanical benefits of controlled braking

Pedestrian ground impact has been categorized into different “mechanisms” defined by the amount of whole body rotation (Crocetta et al., 2015), as summarized in Appendix G. Fig. 10 shows bar plots of the average IC for each ground contact mechanism for both full braking and controlled braking cases combined. The IC variations across mechanism are broadly similar to the vehicle-ground impact speeds trends previously reported by Crocetta et al., 2015, though some differences are present, likely due to the effects of controlled braking present in half

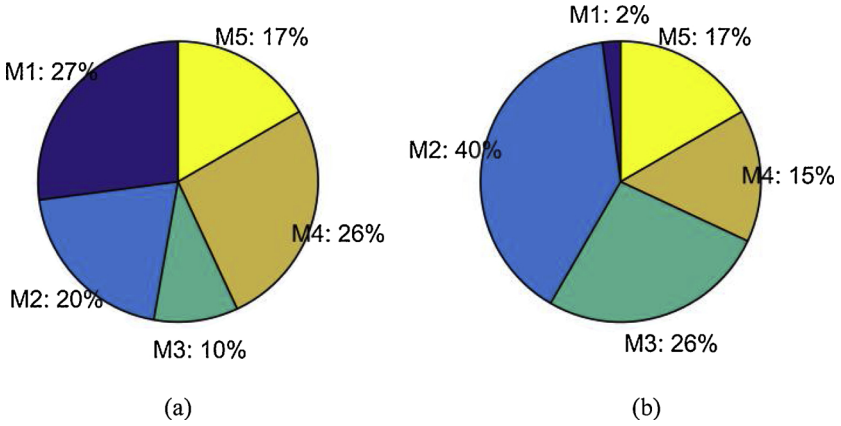

Fig. 11. The proportion of the different mechanisms for (a) full braking compared to (b) controlled braking.

Table 2
Correlation coefficients of braking parameters t_1 and t_2 with collision variables.

	t_1	t_2	Impact speed	Pedestrian gait	Pedestrian size	BLE height
t_1	1	0.248*	−0.692*	0.102	0.283*	−0.556*
t_2	0.248*	1	0.046	0.177	0.265*	−0.320*

* Correlation is significant at the 0.01 level (2-tailed).

the cases. Fig. 11 gives the proportions of each mechanism in the full braking and controlled braking group. The average IC of mechanism 2 is the lowest and its proportion increases from 20% to 40% in the controlled braking group compared to the full braking group. In contrast, the average IC of mechanism 4 is the highest and its proportion decreases from 26% to 15% for controlled braking. These changes illustrate the benefits of controlled braking.

4.3. Correlations between t_1, t_2 and input variables

The times t_1 and t_2 define the proposed controlled braking pulse. Although optimizing these is not the focus of this paper, we do assess correlations between t_1, t_2 and the impact speed, the pedestrian gait and size, and the vehicle shape to guide future evaluation of t_1 and t_2. The Spearman method in SPSS was employed, see Table 2. The time t_1 is of course negatively correlated with impact speed, but a higher BLE also reduces the time to head contact (possibly due to the higher windscreens in vehicles with higher BLEs). The high correlation coefficient implies that t_1 is predictable for future controlled braking algorithms.

As for t_2, though it also has a statistically significant correlation with t_1, the pedestrian size and the vehicle shape, the correlation coefficients are small and predicting t_2 from these parameters alone is difficult. Accordingly, this needs to be a focus of future research. Here, we emphasize that the braking strategy employed (Fig. 3) is not presented as an optimal strategy, but rather a first guess.

5. Conclusions

We used virtual experiments to generate support for the hypothesis that controlled braking mostly reduces the severity of pedestrian ground contact for vehicle shapes where there is a wrap trajectory. Furthermore, controlled braking also increases the proximity of the vehicle to the pedestrian at the instant of ground contact, which may provide opportunities for future vehicle based interventions to cushion ground contact. An assessment of video footage of actual vehicle pedestrian collisions suggests the increased stopping distance associated with controlled braking mostly poses no conflict with the available free space in front of the vehicle, though this needs more detailed assessment in future. Significant further evaluation is required to robustly protect pedestrians for those cases where controlled braking is not of benefit.

Acknowledgement

This work was supported by the National Natural Science Foundation of China (51775056), the Natural Science Foundation of Hunan Province (2018JJ3544) and the China Scholarship Council (CSC).

Appendix A. Contact characteristics for different vehicle front structures

See Fig. A1

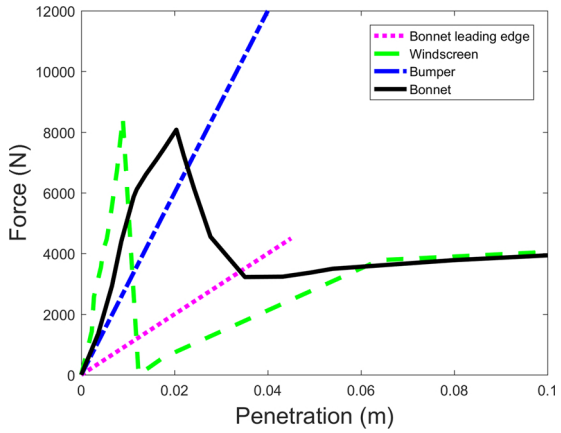

Fig. A1. Force/Penetration curves of contact characteristics for different vehicle front structures.

Appendix B. Brake Pulse Evaluation

B-1 The process of calculating t_1

According to 34 accident cases extracted from Zou et al., 2017, the relationship between t_1 and impact velocity v was obtained, which is

$$t_1 = 0.567 - 0.116 \log(v) \quad \text{(B1)}$$

with a R-square 0.810 and a sigma 0.00. The corresponding figure can be found in Fig. B1. This was used to estimate t_1 according to the impact speed. For $v = 41$ km/h, the regression yields $t_1 = 0.14$ s.

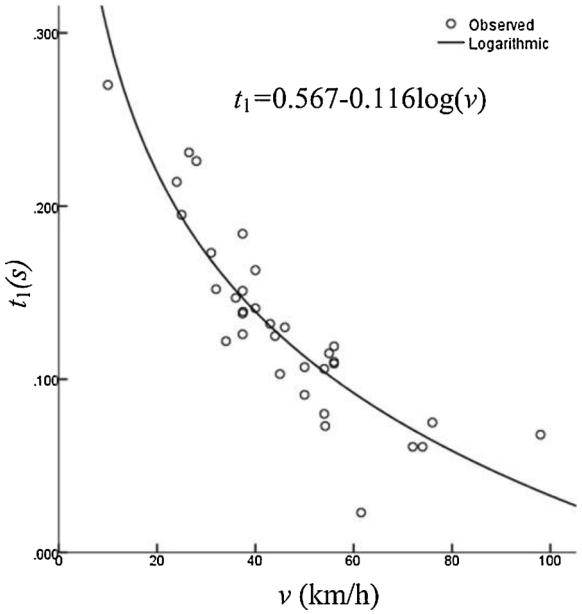

Fig. B1. The relationship between the t_1 and v based on accident cases.

Table B1
Detailed information about those collected accident cases.

No.	Location 1	Location 2	Impact speed (km/h)	Time	AASD (m)
1	City	Curve road	18	Day	6
2	City	Intersection	18	Day	25
3	City	Intersection	18	Day	9
4	City	Pavement	20	Day	10
5	Highway	Straight road	20	Day	80
6	Suburbs	Pavement	20	Day	20
7	City	Pavement	20	Day	15
8	City	Intersection	20	Day	3
9	Suburbs	Straight road	21.6	Day	8
10	City	Intersection	21.6	Day	7
11	Suburbs	Straight road	21.6	Day	10
12	City	Intersection	21.6	Day	5
13	Suburbs	Curve road	23.6	Day	20
14	Suburbs	Straight road	25	Day	5
15	Suburbs	Pavement	25	Day	20
16	City	Pavement	25	Day	8
17	City	Intersection	25	Night	5
18	Suburbs	Pavement	25.2	Day	7
19	Suburbs	Intersection	25.2	Day	5
20	Suburbs	Pavement	26	Night	8
21	City	Intersection	26	Day	9
22	Suburbs	Pavement	28	Day	13
23	City	Pavement	28	Day	1
24	Suburbs	Intersection	28.8	Day	8
25	City	Pavement	28.8	Day	45
26	Suburbs	Straight road	28.8	Day	15
27	City	Pavement	28.8	Day	60
28	Suburbs	Straight road	28.8	Day	10
29	Suburbs	Curve road	28.8	Day	15
30	Suburbs	Intersection	28.8	Day	20
31	City	Pavement	30	Night	20
32	City	Pavement	30	Day	5
33	City	Intersection	30	Day	4
34	Suburbs	Straight road	30	Day	5
35	Suburbs	Intersection	30	Day	0
36	City	Intersection	30	Day	4
37	City	Straight road	30	Night	8
38	City	Straight road	31	Day	18
39	City	Straight road	32.4	Day	15
40	Suburbs	Pavement	32.4	Day	30
41	City	Pavement	33	Day	20
42	City	Pavement	33	Day	20

(*continued on next page*)

Table B1 (*continued*)

No.	Location 1	Location 2	Impact speed (km/h)	Time	AASD (m)
43	Suburbs	Intersection	34	Day	9
44	City	Intersection	34	Day	15
45	City	Intersection	34.6	Day	20
46	Suburbs	Intersection	35	Night	2
47	City	Pavement	35	Day	15
48	Suburbs	Intersection	35	Day	10
49	Suburbs	Straight road	35	Day	15
50	Suburbs	Straight road	36	Day	30
51	Suburbs	Straight road	36	Day	10
52	City	Pavement	36	Day	100
53	City	Pavement	36	Day	40
54	Suburbs	Pavement	38	Day	20
55	City	Intersection	38	Day	2
56	Suburbs	Straight road	39.6	Day	60
57	Suburbs	Intersection	39.6	Day	20
58	City	Intersection	40	Day	8
59	City	Straight road	40	Day	25
60	City	Pavement	40	Day	10
61	City	Pavement	40	Night	20
62	City	Straight road	40	Day	8
63	City	Curve road	40	Day	4
64	City	Straight road	40	Day	20
65	City	Intersection	40	Day	20
66	City	Intersection	40	Night	10
67	City	Intersection	40	Day	0
68	City	Pavement	40	Night	10
69	City	Pavement	42	Day	38
70	City	Intersection	42	Day	18
71	City	Straight road	43	Day	30
72	Suburbs	Straight road	43.2	Day	20
73	Suburbs	Pavement	45	Day	15
74	City	Pavement	45	Day	15
75	Suburbs	Straight road	45	Day	25
75	Suburbs	Straight road	45	Day	20
77	City	Straight road	45	Day	23
78	City	Pavement	47	Night	10
79	City	Pavement	48	Day	25
80	City	Pavement	50	Day	25
81	Suburbs	Intersection	50	Day	5
82	Highway	Tunnel entrance	50	Day	15
83	Suburbs	Pavement	50	Night	20
84	Suburbs	Pavement	50	Night	25
85	City	Pavement	50	Day	25
86	Suburbs	Intersection	52	Day	0
87	Suburbs	Straight road	55	Day	10
88	City	Straight road	55	Day	12
89	Suburbs	Pavement	60	Day	25
90	Suburbs	Pavement	60	Night	25
91	Suburbs	Straight road	64	Day	8
92	Highway	Straight road	65	Night	25
93	Highway	Straight road	65	Day	100
94	Suburbs	Intersection	65	Day	30
95	Highway	Straight road	65	Night	20
96	Highway	Tunnel entrance	70	Day	100
97	City	Intersection	72	Night	15
98	Highway	Straight road	75	Day	100
99	City	Pavement	75	Day	30
100	City	Intersection	75	Day	12

B-2 The maximum value of t_2.

After obtaining t_1, the impact velocity was set to 41 km/h and controlled braking was implemented by changing the value of t_2. Following many trials, we found that the AASD is 20 m when t_2 is 1.4 s. Results are shown in Fig. B2. Hence, we can conclude that the maximum value of t_2 is 1.4 s.

B-3 Detailed information on collected accident cases.

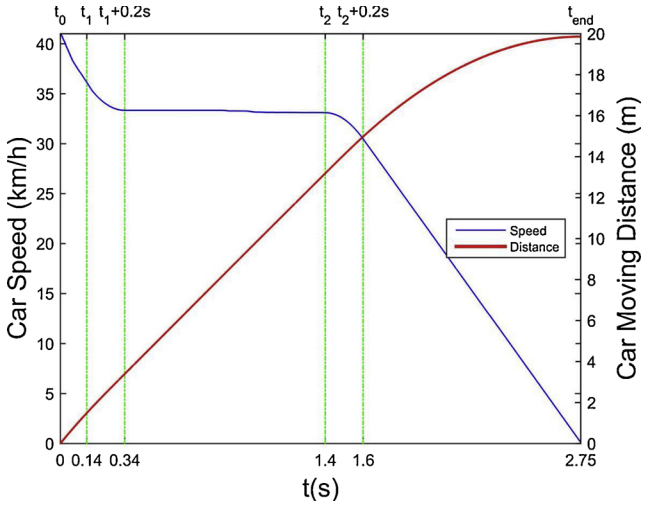

Fig. B2. The relationship between the speed, the moving distance and time.

Appendix C. The difference of HIC versus Car Shape

For different vehicle shapes (average median reduction is 103.9; benefit observed in 65% of cases). See Fig. C1

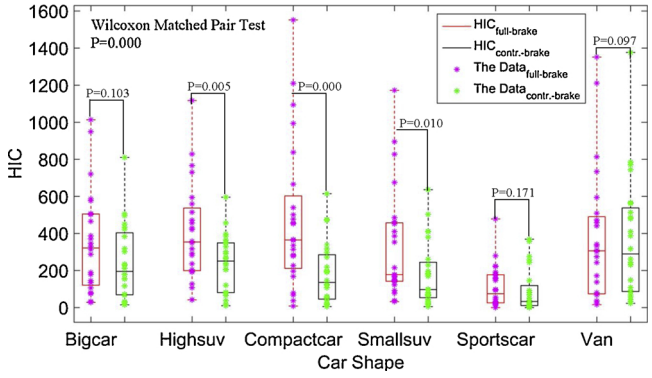

Fig. C1. The difference in HIC score for controlled braking compared to full braking.

Appendix D. The kinematic response of the pedestrian in controlled braking and full braking

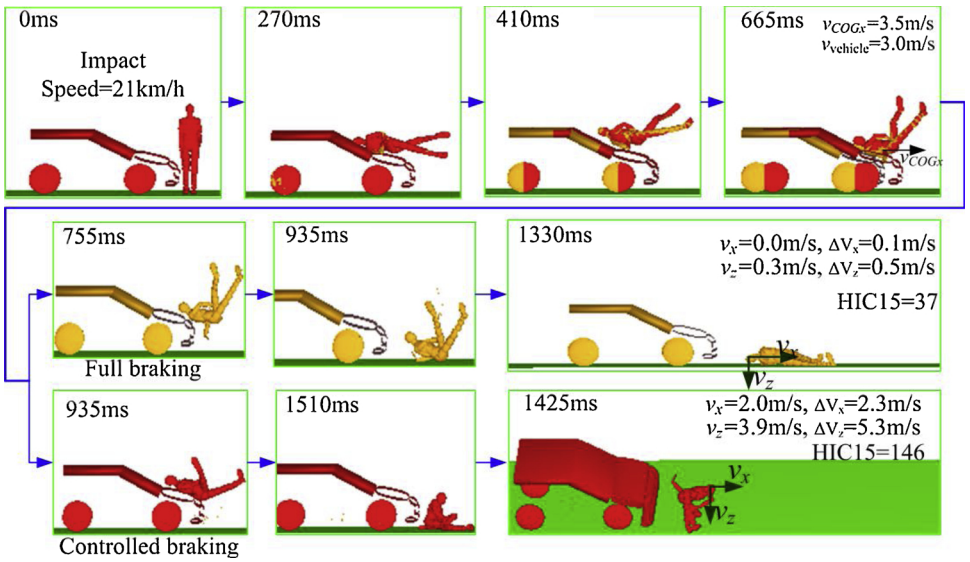

Fig. D1. Sample case where controlled braking (red) does not present an improvement for pedestrian ground contact over full braking (yellow): v_x /v_z are the pedestrian head cg velocity components just prior to ground contact; ΔVx/z are the components of the pedestrian's head cg velocity change during ground impact; $v_{vehicle}$ is the vehicle velocity and v_{COGx} is the horizontal velocity of the pedestrian cg;). The HIC score for controlled braking is slightly higher than for full braking.

Appendix E. Bar plots of WIC versus Velocity and Pedestrian

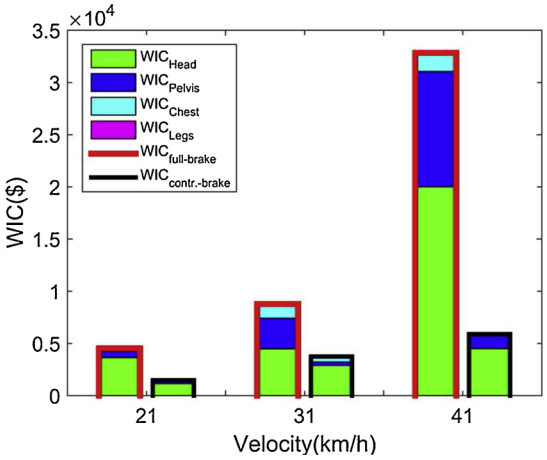

Fig. E1. Bar plots of WIC for full braking versus controlled braking at different impact velocities.

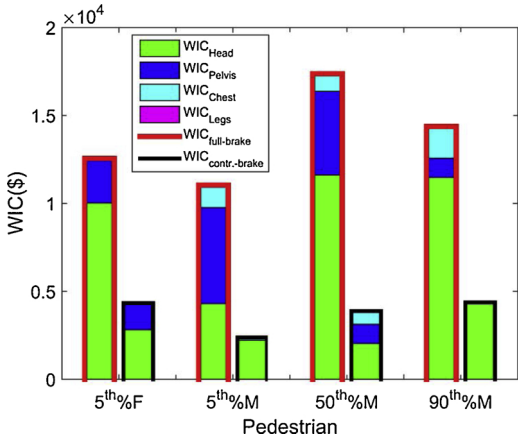

Fig. E2. Bar plots of WIC for full braking versus controlled braking for different pedestrian sizes.

Appendix F. WIC versus Velocity and Pedestrian and different vehicle shapes

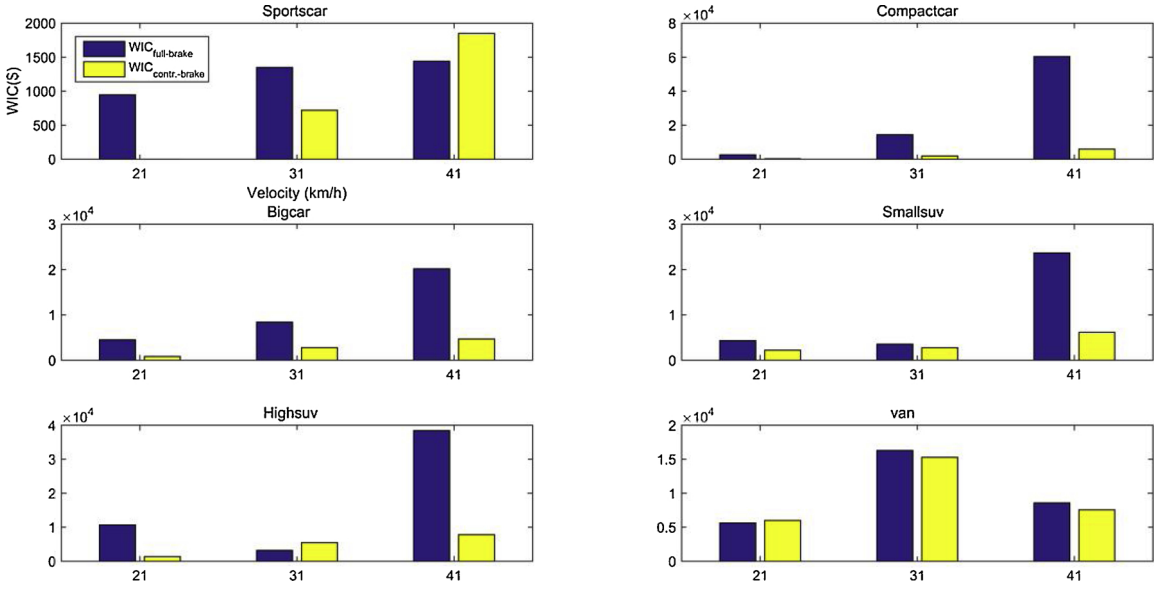

Fig. F1. Bar plots of WIC for full braking versus controlled braking for different vehicle shapes.

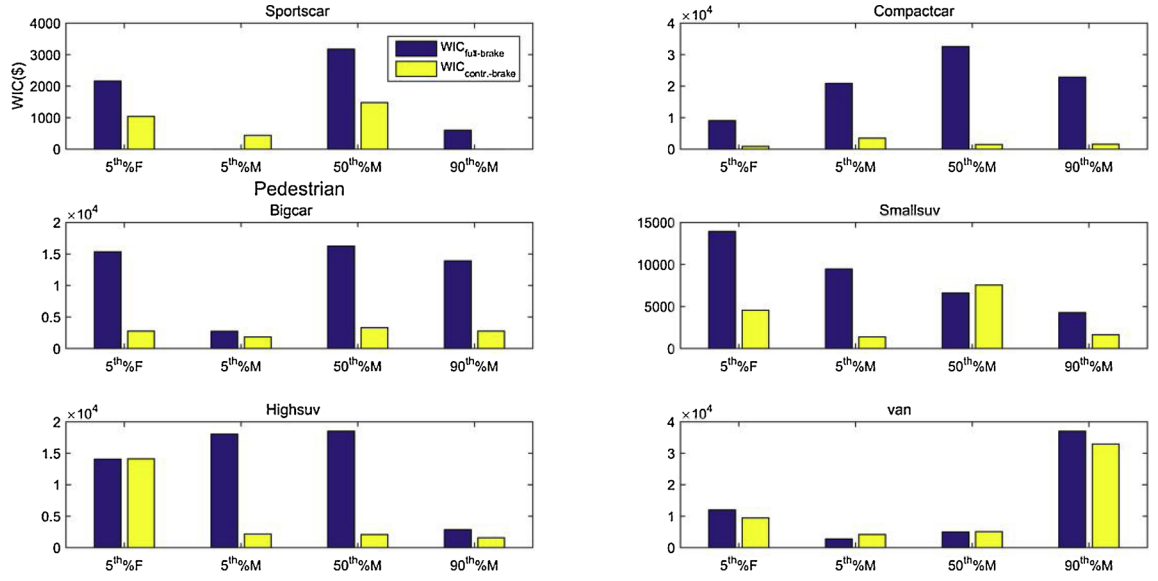

Fig. F2. Bar plots of WIC for full braking versus controlled braking for different vehicle shapes.

Appendix G. Ground contact mechanisms

See Fig. G1

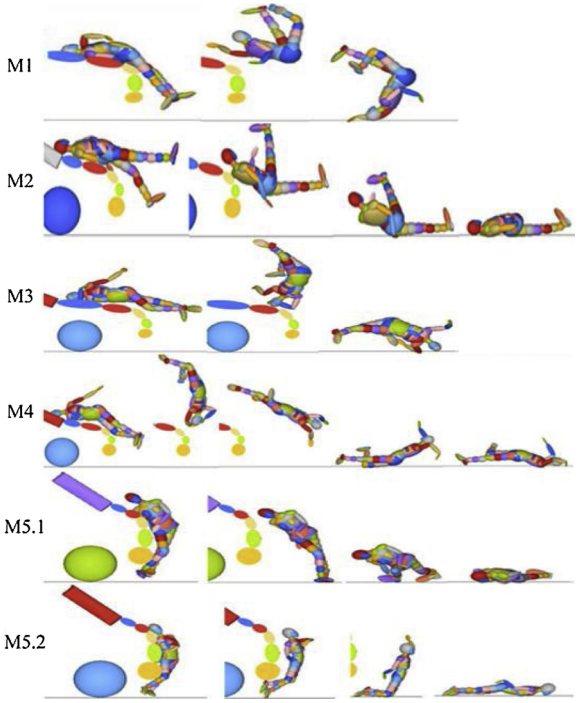

Fig. G1. The 6 proposed ground contact mechanisms of (Crocetta et al., 2015).

References

Badea-Romero, A., Lenard, J., 2013. Source of head injury for pedestrians and pedal cyclists: Striking vehicle or road? Accid. Anal. Prev. 50, 1140–1150.

Brach, R., Brach, R.M., 2005. Vehicle Accident Analysis and Reconstruction Methods. SAE International Publisher, Pennsylvania, USA.

Cavallero, C., Cesari, D., Ramet, M., Billaut, P., J. F, Seriat-Gautier, B., Bonnoit, J., 1983. Pedestrian Safety: Influence of Shape of Passenger Car–Front Structures Upon Pedestrian Kinematics and Injuries: Evaluation Based on 50 Cadaver Tests. Society of Automotive Engineers, SAE Paper No. 830624.

Crocetta, G., Piantini, S., Pierini, M., Simms, C., 2015. The influence of vehicle front-end design on pedestrian ground impact. Accid. Anal. Prev. 79, 56–69.

Datentechnik, Dr.Steffan, 2013. PC-CRASH, A Simulation Program for Vehicle Accidents, Operation and Technical Manual, Version 10.0.

Eubanks, J.J., Cateel, D.A., et al., 2018. Pedestrian Accident Reconstruction and Litigation, third edition. Lawyers and Judges Publishing Company, Tucson Arizona USA.

Feng, C., Wang, F., Chen, X., Wei, F., Liu, S., Yin, Z., 2013. Head dynamic response based on reconstruction of vehicle-pedestrian accidents with the video. Yiyong Shengwu Lixue/J. Medi. Biomechanics 28 (2), 164–170 (In Chinese).

Guillaume, A., Hermitte, T., Hervé, V., Fricheteau, R., 2015. Car or ground: which causes more pedestrian injuries? Proceedings of the 24th International Technical Conference on the Enhanced Safety of Vehicles (ESV).

Hamacher, M., Eckstein, L., Paas, R., 2012. Vehicle related influence of post-car impact pedestrian kinematics on secondary impact. Proceedings of the Proceedings of the International Research Council on the Biomechanics of Injury Conference. pp. 717–729.

Han, Y., Li, Q., Wang, F., Wang, B., Mizuno, K., Zhou, Q., 2019. Analysis of pedestrian kinematics and ground impact in traffic accidents using video records. Int. J. Crashworthiness 24 (2), 211–220. https://doi.org/10.1080/13588265.2018.1429520.

Kendall, R., Meissner, M., Crandall, J., 2006. The Causes of Head Injury in Vehicle-Pedestrian Impacts: Comparing the Relative Danger of Vehicle and Road Surface. SAE Technical Paper 2006-01-0462https://doi.org/10.4271/2006-01-0462.

Khaykin, A., Larner, D.L., 2016. Adhesive Vehicle Front End for Mitigation of Secondary Pedestrian Impact. Google Patents.

Klug, C., 2018. Assessment of Passive Vulnerable Road User Protection With Human Body Models. MSC Thesis. Graz University of Technology, Graz, Austria.

Li, G., 2017b. Optimization of Vehicle Front Shape for Pedestrian Protection. MSC Thesis. Trinity College Dublin, Dublin, Ireland.

Li, G., Yang, J., Simms, C., 2015. The influence of gait stance on pedestrian lower limb injury risk. Accid. Anal. Prev. 85, 83–92.

Li, G., Yang, J., Simms, C., 2016a. A virtual test system representing the distribution of pedestrian impact configurations for future vehicle front-end optimization. Traffic Inj. Prev. 17 (5), 515–523.

Li, G., Otte, D., Yang, J., Simms, C., 2016b. Can a small number of pedestrian impact scenarios represent the range of real-world pedestrian injuries? Proceedings of the International Research Council on Biomechanics of Injury(IRCOBI) Conference.

Li, G., Yang, J., Simms, C., 2017a. Safer passenger car front shapes for pedestrians: a computational approach to reduce overall pedestrian injury risk in realistic impact scenarios. Accid. Anal. Prev. 100, 97–110.

Li, G., Wang, F., Otte, D., Cai, Z., Simms, C., 2018. Have pedestrian subsystem tests improved passenger car front shape? Accid. Anal. Prev. 115, 143–150.

Nie, B., Zhou, Q., 2016. Can new passenger cars reduce pedestrian lower extremity injury? A review of geometrical changes of front-end design before and after regulatory efforts. Traffic Inj. Prev. 17 (7), 712–719.

Otte, D., Pohlemann, T., 2001. Analysis and load assessment of secondary impact to adult pedestrians after car collisions on roads. Proceedings of the International Research Council on Biomechanics of Injury (IRCOBI) Conference.

Peng, Y., Deck, C., Yang, J., Willinger, R., 2012. Effects of pedestrian gait, vehicle-front geometry and impact velocity on kinematics of adult and child pedestrian head. Int. J. Crashworthiness 17 (5), 553–561.

Pipkorn, B., Fredriksson, R., Olsson, J., 2007. Bumper bag for SUV to passenger vehicle compatibility and pedestrian protection. 20Th International Technical Conference on the Enhanced Safety of Vehicles (ESV).

Shang, S., Otte, D., Li, G., Simms, C., 2018a. Detailed assessment of pedestrian ground contact injuries observed from in-depth accident data. Accid. Anal. Prev. 110, 9–17.

Shang, S., Masson, C., Arnoux, P.J., Py, M., Simms, C., 2018b. Preliminary assessment of the MADYMO pedestrian model for predictiong pedestrian Ground contact kinematics. 2018 IRCOBI Conference Proceedings.

Shi, L., Han, Y., Huang, H., Li, Q., Wang, B., Mizuno, K., 2018. Analysis of pedestrian-to-ground impact injury risk in vehicle-to-pedestrian collisions based on rotation angles. J. Safety Res. 64, 37–47.

Simms, C.K., Wood, D.P., 2006a. Effects of pre-impact pedestrian position and motion on kinematics and injuries from vehicle and ground contact. Int. J. Crashworthiness 11 (11), 345–355.

Simms, C., Wood, D., 2009. Pedestrian and cyclist impact. Solid Mech. Appl. 166, 31–49.

Simms, C.K., Ormond, T., Wood, D.P., 2011. The influence of vehicle shape on pedestrian ground contact mechanisms. Proceedings of the Proceedings of IRCOBI Conference.

Stcherbarcheff, G., Tarriere, C., Duclos, P., Fayon, A., Got, C., Patel, A., 1975. Simulation of collisions between pedestrians and vehicles using adult and child dummies. Society of Automotive Engineers, SAE Paper No. 751167.

Tamura, A., Duma, S., 2011. A study on the potential risk of traumatic brain injury due to ground impact in a vehicle-pedestrian collision using full-scale finite element models. Int. J. Veh. Saf. 5 (2), 117–136.

Tamura, A., Koide, T., Yang, K.H., 2014. Effects of ground impact on traumatic brain injury in a fender vault pedestrian crash. Int. J. Veh. Saf. 8 (1), 85–100.
WHO, 2013. Global Status Report on Road Safety 2013: Supporting a Decade of Action. World Health Organization.
Yin, S., Li, J., Xu, J., 2017. Exploring the mechanisms of vehicle front-end shape on pedestrian head injuries caused by ground impact. Accid. Anal. Prev. 106, 285–296.
Zou, T., Yu, Z., Cai, M., Liu, J., 2011. Analysis and application of relationship between post-braking-distance and throw distance in vehicle-pedestrian accident reconstruction. Forensic Sci. Int. 207 (1-3), 135–144.
Zou, T., Xiao, J., Hu, L., Li, H., Cai, M., 2017. Human-body injury sources and correlation analysis on car-pedestrian accidents. Automotive Engineering 39 (7), 748–753 (In Chinese).